CONFERENCE PRE-PRINT

NEW UNDERSTANDING OF RESONANT LAYER RESPONSE VIA EXTENDED DRIFT MHD

Implications of high order physics on application of resonant magnetic perturbations

J.K. Park Seoul National University Seoul, South Korea Email: jkpark@snu.ac.kr

Y.S. Lee Seoul National University Seoul, South Korea

J. Waybright Princeton University Princeton, New Jersey, USA

N. C. Logan Columbia University New York, New York, USA

Abstract

Notable progress has been recently achieved in understanding and predicting resonant layer response under non-axisymmetric magnetic perturbations in tokamaks, by incorporating high order physics into the two-fluid drift-MHD layer model. First, electron viscosity is shown to play an important role in low torque plasmas even despite its smallness, since the generalized Ohm's law requires a delicate balance with electron dynamics. This leads to a stronger density scaling of field penetration threshold than earlier work, consistent with locked mode experiments. Secondly, the perturbation in ion flow is shown to be critical in high- β conditions by maintaining screening effects, shifting the natural rotating frequency. As a result, electromagnetic torque remains finite even when electron flow becomes stationary without field penetration – a surprising prediction for reactor-relevant regimes. The incorporation of these two elements concludes the two-fluid drift MHD physics implication for the narrow resonant layer response in linear regimes, as will be reviewed in this paper. The aforementioned results have been verified by outstanding agreements between the extended asymptotic matching theory and computations based on Riccati transformation. These new elements for layer model are being integrated to the general perturbed equilibrium framework to develop a reliable predictive model for field penetration thresholds – a central subject of error field correction against locked modes and resonant magnetic perturbation (RMP) ELM suppression.

1. INTRODUCTION

Field penetration is a bifurcation process in which magnetic islands form and grow near the resonant surfaces in response to non-axisymmetric magnetic perturbations [1]. This involves a major alteration of magnetic topologies of nested flux surfaces in a tokamak and thus significantly affect pressure or current profiles and thereby various instabilities. The field penetration is believed to be the key to understanding the effects of an intrinsic error field (EF) or a controllable resonant magnetic perturbation (RMP) [2]. When the field penetration happens in low (m,n) rational surfaces due to EFs, it can lead to a disruptive locked mode. If it is induced by RMPs with higher (m,n) rational numbers, island-driven transport can reduce the steepness in the edge profiles below the instability boundary of edge-localized modes (ELMs) [3]. One of the critical questions for EF correction (EFC) and RMP ELM suppression is to determine the onset point, such as field penetration threshold in terms of the resonant field amplitudes, just before the bifurcation occurs.

The prediction of field penetration thresholds requires resolving complex boundary layer phenomena near the rational surfaces. One of the best theoretical approaches to incorporate extended physics is the asymptotic matching for the narrow

resonant layers, as it has been pioneered by R. Fitzpatrick et al [4, 5, 6]. Assuming the region outside the layer (outer layer) is governed by ideal MHD, a magnetic perturbation can be determined in outer layers provided the so-called Δ parameter. Particularly in the linear phase, which includes the onset point of the field penetration, the layer response is in fact completely characterized by Δ . As well known since the tearing mode was analyzed first by Furth-Killeen-Rosenbluth (FKR), Δ represents the screening currents within the layer preventing the resonant field and must be equivalent to $\Delta_{in} = [d \ln \psi/dx]_{-}^{+}$ across the layer where ψ is the helical flux. These screening currents create an electromagnetic torque $\delta \vec{j} \times \delta \vec{B}$, slowing down rotation against viscous restoring torque and increasing $\delta \vec{j} \times \delta \vec{B}$ rapidly towards the so-called natural frequency. The linear assumption breaks down at this point, involving nonlinearly growing islands, where we define the onset of field penetration.

Earlier theories based on a slab representation had been extended successfully to identify 10 distinct drift-MHD regimes, highlighting the complexity of layer response. Unfortunately, none of these regimes show the scaling characteristics observed in the field penetration threshold due to EFs, sparking extensive discussions on the effects of nonlinearlity [7]. Nevertheless, some of scaling such as the strong correlation with density n_e or toroidal field B_T appears to be more universal than what would be expected when it occurs only in nonlinear regimes. This motivates our recent work on extended two-fluid drift-MHD in linear phase as described here. There are two new elements in this extension; electron viscosity and parallel ion flow. The electron viscosity μ_e is often ignored compared to the ion viscosity μ_i , assuming classically $\mu_e/\mu_i \sim \sqrt{m_e/m_i}$. This is appropriate for ion dynamics, but not electron dynamics, since the electron viscosity competes with other small effects such as resistivity, not with the ion viscosity. Indeed the electron viscosity turns out to be critical in the parametric scaling for high viscous regime which is relevant for most of tokamak operations [8, 9]. The incorporation of the parallel ion flow is shown to be more instrumental in layer response not only because it shifts the natural frequency but also it resolves the singularity near the natural frequency in linear regimes [10]. This effect becomes more prominent when plasma β increases and ion gyroradius decreases, or $(c_\beta/D)^2$ as will be described later, and may prohibit the field penetration entirely - a surprising outcome.

The modeling extension has been conducted in three different approaches. First, analytic treatments are used whenever it remains tractable, by asymptotic matching in Fourier space. It is possible to include electron viscosity relatively in a straightfoward manner but it requires multiple layer divisions in case of parallel ion flow. When it is possible to couple the system of equations in Fourier space, a Riccati transformation is used to estimate the Δ more accurately while verifying analytic predictions. The full inclusion of parallel flow effects is done only numerically in configuration space, but some of its key ingredients such as the natural frequency shift are also remarkably verified by new analytic methods. The full layer solver is implemented under SLAYER code [11], which has been integrated to the GPEC code package for the prediction of field penetration threshold in actual experiments. Here we will present a part of experimental applications using only the local parameters for a limited dataset, but it is possible to apply this framework for the field penetration threshold database with fully reconstructed profiles as it has been recently attempted for RMP ELM suppression [12].

This paper is organized as follows. First our theoretical background of drift-MHD model to evaluate Δ and field penetration thresholds will be summarized in Sec. 2. Sec. 3 will highlight new physics understanding along with electron viscosity and its parametric dependencies, and also ion parallel flow which can strongly screen field penetration process. Sec. 4 will show the experimental applications for locked mode threshold database of Ohmically heated cases, with local parameters as well as implication to parametric scaling projection.

2. THEORETICAL BACKGROUND OF DRIFT-MHD LAYER MODEL

2.1. Linearized drift-MHD equations

The drift-MHD model in a narrow slab layer has been developed for magnetic field $\vec{B} = \vec{\nabla} \psi \times \hat{z} + (B_0 + Z(1+\tau)/d_i)\hat{z}$ and flow $\vec{V} = \vec{\nabla} \phi \times \hat{z} + V_z \hat{z}$, where B_0 is a constant magnetic field along the symmetry direction \hat{z} , $\tau = T_i/T_e$, ion skin depth $d_i \equiv \sqrt{m_i/n_0 e^2 \mu_0}/a$ with minor radius a. The radial direction is represented by $x = r - r_s$ with r is the radial flux label and $r = r_s$ is the radial position of the resonant surface having q = m/n. Linearizing $\hat{z} \cdot \text{and } \hat{z} \cdot \vec{\nabla} \times \text{component from the generalized Ohm's law, and <math>\hat{z} \cdot \vec{\nabla} \times \text{component from ion momentum equation combined with the pressure evolution, respectively, against a perturbation <math>\propto e^{i(m\theta - n\phi)} = e^{iky}$, one can obtain:

$$ix(\tilde{Z} - \tilde{\phi}) = i\epsilon(Q_e - Q)\tilde{\psi} + \epsilon^3 \left(\nabla^2 \tilde{\psi} - (1 + \tau)P_e \nabla^2 \tilde{V}_z\right) - \epsilon^5 (1 + \tau)P_e \frac{D^2}{c_\beta^2} \nabla^4 \tilde{\psi},\tag{1}$$

$$ic_{\beta}^{2}x\tilde{V}_{z} = i\epsilon(Q\tilde{Z} - Q_{e}\tilde{\phi}) - i\epsilon^{2}D^{2}x\nabla^{2}\tilde{\psi} - \epsilon^{3}C^{2}\nabla^{2}\tilde{Z} - \epsilon^{5}P_{e}D^{2}(\nabla^{4}\tilde{\psi} - \nabla^{4}\tilde{Z}), \tag{2}$$

$$ix\nabla^2 \tilde{\psi} = i\epsilon (Q - Q_i)\nabla^2 \tilde{\psi} - \epsilon^3 \left(P\nabla^4 (\tilde{\psi} + \tau \tilde{Z}) + P_e \nabla^4 (\tilde{\psi} - \tilde{Z}) \right), \tag{3}$$

$$ix\tilde{Z} = i\epsilon(Q\tilde{V}_z + Q_e\tilde{\psi}) - \epsilon^3(P + P_e)\nabla^2\tilde{V}_z - \epsilon^5 P_e \frac{D^2}{c_\beta^2}\nabla^4\tilde{\psi}.$$
 (4)

This constitutes the so-called four-field model for the perturbed (ψ, Z, ϕ, V_z) . It is clear that the solutions to the leading order $\mathcal{O}(1)$ are given by $\tilde{Z} = \tilde{\phi} = \tilde{V}_z = 0$ and $\nabla^2 \tilde{\psi} = 0$, except x = 0 which exhibits the boundary layer phenomena. In a

slab geometry near x=0, $\nabla^2 \tilde{\psi}=d^2 \tilde{\psi}/dx^2-k^2x=0$. The solution of this ideal outer-layer equation asymptotes linearly towards the boundary layer by

$$\lim_{x \to 0} \left[\frac{\Delta}{\psi_{mn}} + \Delta' \right] \to \left[\frac{d \ln \psi}{dx} \right]_{-}^{+} \leftarrow \lim_{X \to \infty} \Delta_{in}. \tag{5}$$

Here the LHS represents the $[d \ln \psi/dx]_-^+$ from the outer layer, including the contributions from the external perturbation (such as EF or RMP) Δ and from the internal perturbation Δ' which is often named tearing mode index. The small parameter is defined as $\epsilon \equiv (\eta/k)^{1/3} = r_s S^{-1/3}$ with the Lundquist number S. The set of parameter $(Q,Q_e,Q_i,c_\beta,C^2,D,P,P_e)$ is normalized accordingly, representing $\vec{E} \times \vec{B}$ rotation (including the linear growth rate) by Q, electron and ion diamagnetic rotation by Q_e and Q_i , plasma β by c_β , conductivity (or diffusivity) by C^2 , ion skin depth (or ion gyro-radius) by D, ion and electron viscosity by P and P_e , respectively. Note that $C^2 = c_\beta^2 + (1 - c_\beta^2)K$ where K is the conductivity. Recent work by R. Fitzpatrick also includes the perpendicular diffusivity P_\perp [13] which becomes identical to our formulation by letting $C^2 = P_\perp$. The viscosities and conductivity scale as $\mathcal{O}(\epsilon^3)$ whereas all the others (except c_β) scale linearly with $\mathcal{O}(\epsilon)$. Here we essentially follow the asymptotic principle of maximal complexity to keep all relevant information in the layer treatments.

Using the stretch variable for the layer $x = \epsilon X$, one can obtain the full linear drift-MHD equations:

$$i(Q - Q_e)\tilde{\psi} = iX(\tilde{\phi} - \tilde{Z}) + \frac{d^2\tilde{\psi}}{dX^2} - (1 + \tau)P_e\left(\frac{d^2\tilde{V}_z}{dX^2} + \frac{D^2}{c_\beta^2}\frac{d^4\tilde{\psi}}{dX^4}\right),\tag{6}$$

$$iQ\tilde{Z} = iQ_{e}\tilde{\phi} + iD^{2}X\frac{d^{2}\tilde{\psi}}{dX^{2}} + ic_{\beta}^{2}X\tilde{V}_{z} + \left(c_{\beta}^{2} + (1 - c_{\beta}^{2})K\right)\frac{d^{2}\tilde{Z}}{dX^{2}} + P_{e}D^{2}\left(\frac{d^{4}\tilde{\phi}}{dX^{4}} - \frac{d^{4}\tilde{Z}}{dX^{4}}\right),\tag{7}$$

$$i(Q - Q_i)\frac{d^2\tilde{\phi}}{dX^2} = iX\frac{d^2\tilde{\psi}}{dX^2} + P\left(\frac{d^4\tilde{\phi}}{dX^4} + \tau\frac{d^4\tilde{Z}}{dX^4}\right) + P_e\left(\frac{d^4\tilde{\phi}}{dX^4} - \frac{d^4\tilde{Z}}{dX^4}\right),\tag{8}$$

$$iQ\tilde{V}_z = -iQ_e\tilde{\psi} + iX\tilde{Z} + (P + P_e)\frac{d^2\tilde{V}_z}{dX^2} + P_e\frac{D^2}{c_a^2}\frac{d^4\tilde{\psi}}{dX^4}.$$
 (9)

These equations will determine ψ and thus Δ_{in} by

$$\tilde{\psi}(-X) = \tilde{\psi}(X) \to \psi_{mn} \left[1 + \frac{\hat{\Delta}}{2} |X| + \mathcal{O}\left(\frac{1}{X}\right) \right], \tag{10}$$

where $\hat{\Delta} = \epsilon \Delta_{in}$. This problem is highly steep due to the exponential (or oscillatory) behaviors in the infinite domain $X \in (0, \infty)$, but has been successfully solved based on the matrix Riccati transformation. The full procedure is well documented in [10] and thus we will present only its major implications in Sec. 3.2.

2.2. Fourier and Riccati Transforms

The set of equations can be further simplified by Fourier transform, from a field $\tilde{F}(p) = (\tilde{\psi}, \tilde{Z}, \tilde{\phi}, \tilde{V}_z)$ to $\bar{F} = (\bar{\psi}, \bar{Z}, \bar{\phi}, \bar{V}_z)$ with $\bar{F} = \int_c \tilde{F}(X)e^{ipX}dX$. This becomes particularly useful in the condition where \tilde{V}_z can be ignored. The $P_e d^2 \tilde{V}_z / dX^2$ in Eq. (6) can be ignored simply when $P_e \ll (Q + Pp_*^2)^2 / Pp_*^4$, compared the he last term, and $c_\beta^2 X \tilde{V}_z$ can be ignored when $c_\beta^2 / D^2 \ll (P_e / P) p_*^4 (Q + Pp_*^2)^2$. Although it depends on layer width p_* in p-space, the two conditions are easily met in low Q by $P_e \ll P$ and $c_\beta^2 / D^2 \ll P_e P$ except in very high β condition. Then one can arrive at the three-field equation [8]:

$$i(Q - Q_e)\bar{\psi} = \frac{d(\bar{\phi} - \bar{Z})}{dp} - p^2\bar{\psi} - p^4P_e\frac{D^2}{c_\beta^2}(1+\tau)\bar{\psi},\tag{11}$$

$$iQ\bar{Z} - iQ_e\bar{\phi} = -D^2\frac{d^2(p^2\bar{\psi})}{dp^2} - c_\beta^2 p^2\bar{Z} + P_eD^2 p^4(\bar{\phi} - \bar{Z}),$$
 (12)

$$i(Q - Q_i)p^2\bar{\phi} = \frac{d(p^2\bar{\psi})}{dp} - Pp^4(\bar{\phi} + \tau\bar{Z}) - P_e p^4(\bar{\phi} - \bar{Z}).$$
(13)

Here we also ignore K but in case with high conductivity or high perpendicular viscosity, one can simply replace $c_{\beta} \to C$ in Eq. (12). These equations can be analytically solved since they are combined by the 2nd order ODE with the new variable $Y \equiv \bar{\phi} - \bar{Z}$ by:

$$\frac{d}{dp} \left[\frac{p^2}{\frac{D^2(\tau+1)P_e}{c_\beta^2} p^4 + p^2 + i(Q - Q_e)} \frac{dY}{dp} \right] - p^2 G(p)Y = 0, \tag{14}$$

which G(p) given by, with $P + P_e \cong P$ [9],

 $G(p) = \frac{PP_e D^2(\tau + 1)p^6 + \left(iP_e D^2(Q - Q_i) + Pc_\beta^2\right)p^4 + i(c_\beta^2 + P)(Q - Q_i)p^2 - Q(Q - Q_i)}{PD^2(\tau + 1)p^4 + \left(i(Q - Q_i)D^2 + c_\beta^2\right)p^2 + i(Q - Q_e)}.$ (15)

It is already shown that the proper matching condition for the outer layer is $Y \to Y_0(1+\hat{\Delta}/\pi p)$ [6]. As it stands, this equation for Y(p) is not fully analytically tractable but can be studied asymptotically in each parametric regime. For comparison, we also developed a numerical scheme to solve the Eq. (14) based on a Riccati transformation W=(p/Y)dY/dp, resulting:

$$\frac{dW}{dp} = W \left(\frac{\frac{4D^2 p^3 (\tau + 1) P_e}{c_{\beta}^2} + 2p}{\frac{D^2 p^4 (\tau + 1) P_e}{c_{\beta}^2} + i(Q - Q_e) + p^2} - \frac{1}{p} \right) - \frac{W^2}{p} + pG(p) \left(\frac{D^2 p^4 (\tau + 1) P_e}{c_{\beta}^2} + i(Q - Q_e) + p^2 \right). \tag{16}$$

The Riccati transformation removes the exponential behavior of the solutions and enhances the numerical reliability. The asymptotic behavior of physically relevant solution becomes $W \to -1$ and $dW/dp \to \pi/\hat{\Delta}$ as $p \to +0$. We will present first new analytic results for electron viscosity based on Eq. (14) while numerically validating the asymptotic behaviors based on Eq. (16), and then show the full numerical results based on Eqs. (6-9) to include parallel ion flow effects.

2.3. Torque balance and resonant field penetration

Asymptotic matching between inner and outer region implies a finite helical flux ψ_{mn} and thus islands, inducing an electromagnetic torque which in turn slows down rotation Q from an equilibrium value Q_0 against the viscous torque. The slab model predicts that this balance is no longer possible when the resonant field is larger than a threshold and that the ψ_{mn} can grow indefinitely. In the slab model, this field penetration threshold is predicted as

$$\delta_{crit} = \left[\frac{b_r(r_s)}{B_\phi}\right]_{crit}^2 = \max\left[\frac{2P(Q_0 - Q)}{S\hat{\kappa}} \times \frac{|\hat{\Delta}(Q) - \hat{\Delta}'|^2}{\text{Im}[\hat{\Delta}(Q)]}\right],\tag{17}$$

where $\hat{\kappa} \sim \mathcal{O}(1)$ is a toroidal correction factor for viscosity [6]. The second part of RHS represents the inverse of the electromagnetic torque, $\tau_{\phi} \propto -\mathrm{Im}[\hat{\Delta}(Q)]/|\hat{\Delta}(Q) - \hat{\Delta}'|^2$. Ignoring $\hat{\Delta}' \ll 1$ as often assumed for tearing-stable case, the electromagnetic torque is given by $\tau_{\phi} \propto \mathrm{Im}(1/\hat{\Delta})$. One can see $\tau_{\phi} \to \infty$ in $\hat{\Delta} = 0$ which occurs at $Q = Q_e$ essentially in all regimes when Q slows down, as called a natural frequency. As will be shown, however, the inclusion of parallel flow removes this singularity by leaving $\mathrm{Re}[\hat{\Delta}] \neq 0$ even if $\mathrm{Im}[\hat{\Delta}] = 0$.

Eq. (17) can be analytically estimated if $\hat{\Delta}$ is given, in terms of $(Q,Q_e,Q_i,c_\beta,C,D,P,P_e)$. One can then obtain scaling in terms of dimensionless physical parameters or operational parameters by $Q=S^{1/3}\omega_E\tau_H,\ Q_{i(e)}=-S^{1/3}\omega_{i(e)*}\tau_H,$ $C=c_\beta=\sqrt{\beta/(1+\beta)},\ D=S^{1/3}\rho_s/r_s,\ P=\tau_R/\tau_V=\sqrt{m_i/m_e}P_e$, with $E\times B$ angular frequency ω_E , ion (electron) diamagnetic frequency $\omega_{i(e)*}$, ion Larmor radius with electron temperature ρ_s . The hydrodynamic, resistive, and viscous time scales, τ_H,τ_R , and τ_V are also defined appropriately in the slab. It is of great interest to predict and reproduce the empirical form of parametric scaling $[b_r(r_s)/B_\phi]_{crit}\sim n_e^{\alpha n}T_e^{\alpha T}B_\phi^{\alpha B}R_0^{\alpha R}$ as will be described in the rest of sections.

3. UNDERSTANDING OF HIGH-ORDER MHD EFFECTS

3.1. Electron viscosity and parametric scaling

Earlier work without electron viscosity and parallel ion flow effects identified 10 different regimes [4]. Two nonconstant- ψ regimes with high rotation are Inertial (I) and Visco-Inertial (VI) regimes. Eight constant- ψ regimes are a pair of Resistive-Inertial regimes (RIi,RIii), Visco-Resistive regimes (VRi,VRii), Semi-Collisional regimes (SCi,SCii) and Hall-Resistive regimes (HRi,HRii). In particular, two most relevant regimes for fusion with P>1 and low Q are shown to be SCi and HRi. An issue is that neither of two is consistent with the well-known strong density and inverse- B_{ϕ} scaling. It is the electron viscous effect that shows the empirically feasible scaling for the first time, even if one follows the classical assumption as $P_e = \sqrt{m_e/m_i}P$ [8]. The modified SCi regime by electron viscosity is identified in the limit of $(D^2(\tau+1)P_e/c_{\beta}^2)p^2\gg 1$ and $Q\gg P_eD^2p^4$. Then, Eq. 14 reduces to

$$\frac{d}{dp} \left[\frac{1}{p^2} \frac{dY}{dp} \right] - i P_e \frac{Q - Q_i}{c_\beta^2} Y \approx 0. \tag{18}$$

This form is known as Emden-Fowler differential equation and can be analytically solved, giving

$$\hat{\Delta}_{SCiPe} = \frac{3\Gamma(1/4)i^{7/4}\pi c_{\beta}^{1/2}(Q - Q_e)(Q - Q_i)^{3/4}}{8\Gamma(7/4)D^2(\tau + 1)P_e^{1/4}}.$$
(19)

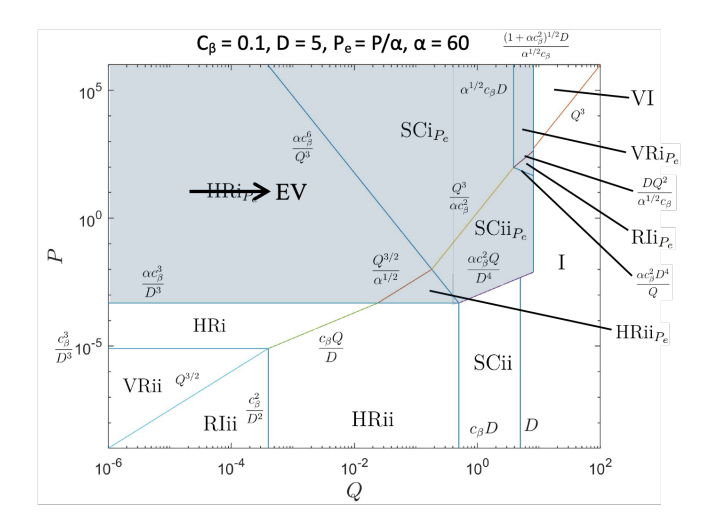


FIG. 1. Q-P space map identifying the different parameter regimes with $c_{\beta}=0.1$, D=1, $Q_e=-Q_i=Q/2$, and $P_e=\sqrt{m_e/m_D}P=P/\alpha$. New regimes with electron viscosity are shown in gray.

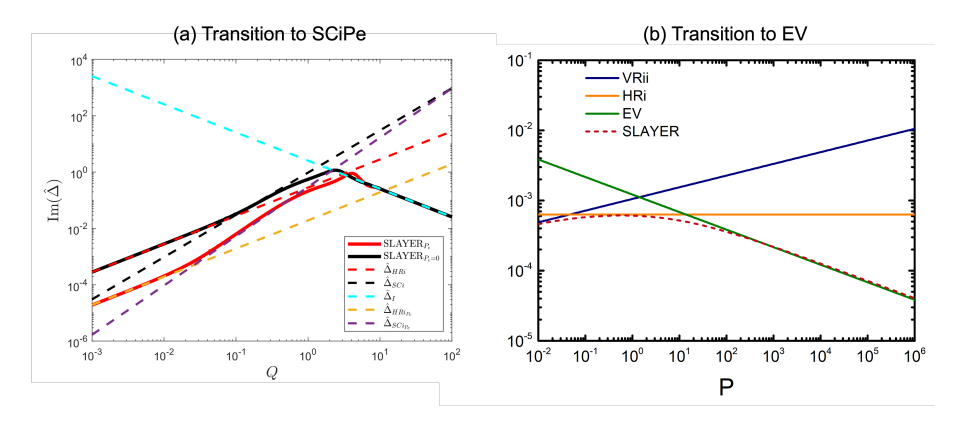


FIG. 2. (a) Transition across HRi, SCi, and I regimes in Q-space showing the asymptotic predictions and SLAYER results in each regime for both including ($P_e \neq 0$) and neglecting ($P_e = 0$) electron viscosity. Here, $c_{\beta} = 0.1$, D = 1, $Q_e = -Q_i = Q/2$, and P = 10. Taken from Ref. [8]. (b) Transition from the VRii to HRi, and to EV regime. $Q = 10^{-3}$, $Q_e = -Q_i = Q/2$, D = 0.2, $C_{\beta} = 0.1$ and $C_{\beta} =$

Notably, this regime is driven only by electron viscosity in the parallel Ohm's law, Eq. (11). The modified HRi regime by electron viscosity, HRiPe, has also been resolved when assuming electron viscosity only in the parallel Ohm's law, but it is quickly shown that the main correction for HRi should arise from electron viscosity in the nonparallel Ohm's law, Eq. (12). This is named the electron-viscous (EV) regime in the limit of $(D^2(\tau+1)P_e/c_\beta^2)p^2 \gg 1$ [9]. Eq. (14) reduces to

$$\frac{d}{dp} \left[\frac{1}{p^2} \frac{d\bar{Y}}{dp} \right] - \frac{D^2(\tau + 1)P_e^2}{c_\beta^2} p^4 \bar{Y} \approx 0$$
(20)

and results in

$$\hat{\Delta}_{EV} = \frac{3i\pi\Gamma(5/8)c_{\beta}^{5/4}(Q - Q_e)}{8^{3/4}\Gamma(11/8)D^{5/4}(\tau + 1)^{5/8}P_e^{1/4}}.$$
(21)

Fig. 1 illustrates the new SCiPe and EV regimes in the limit of large P and small Q. Note that other new regimes such as VRiPe, RiPe, SCiiPe are also shown. They are however narrowly spaced and less significant, and also need to be updated by electron viscosity in non-parallel Ohm's law. These asymptotic results are numerically verified against SLAYER numerical calculations, as illustrated by the two graphs in Fig. 2. In both (a) and (b), one can see that each asymptotic regime is precisely reproduced by numerical SLAYER results as a function of (a) rotation or (b) viscosity.

The parametric dependencies of field penetration threshold are also significantly modified from the earlier ones, as sum-

marized here.

$$\delta_{c,SCi} \sim n^{1/4} T_e^{1/8} B_{\phi}^{-5/4} R_0^{-1} \longrightarrow \delta_{c,SCiPe} \sim n_e^{5/8} T_e^{1/16} R_0^{-3/4} B_{\phi}^{-13/8}$$
(22)

$$\delta_{c,HRi} \sim n^{1/4} T_e^{1/8} B_{\phi}^{-5/4} R_0^{-1} \longrightarrow \delta_{c,HRiPe} \sim n_e R_0^{-1/2} B_{\phi}^{-2} \longrightarrow \delta_{c,EV} \sim n_e^{11/16} T_e^{-5/8} R_0^{1/8} B_{\phi}^{-3/4}$$
 (23)

An important change with electron viscosity is seen particularly in density scaling $\alpha_n=0.6\sim0.7$ which is stronger than the previous SCi or HRi scaling. The stronger density scaling is consistent with longstanding experimental observations. Note that there are still gaps from other empirically known scaling, for example, the so-called 2017 ITPA Ohmic scaling $\delta_c \sim n_e^{1.4} R_0^{0.81} B_T^{-1.8} \beta_N^{-0.86}$ in Ref. [14]. However, if one scales $\beta_N \propto n_e T_e B_T^{-1} R_0$ by fixing the aspect ratio (note there is a typo for the same argument in Ref. [14]), the 2017 scaling becomes $\delta_c \sim n^{0.54} T_e^{-0.86} R_0^{-0.05} B_T^{-0.94}$, close to the EV regime scaling. This scaling for density and B_ϕ is also surprisingly close to new empirical scaling over the full database including L and H modes [15]. Nonetheless, the inter-parametric dependencies as well as the regimes of each data point can be widely different from a device to another, and thus this simple comparison based on a single asymptotic limit is not always appropriate.

3.2. Ion parallel flow shielding for field penetration

In high-beta condition, it may be no longer $c_{\beta}^2/D^2 \ll (P_e/P)p_*^4(Q+Pp_*^2)^2$ and then becomes necessary to include \bar{V}_z . The four-field model including this perturbed ion parallel flow has been successfully developed as described in detail by Ref. [10] and recently incorporated into SLAYER code. This full solver in configuration space verifies various asymptotic limits as well as the reduced Riccati scheme in the momentum space. In addition, it is shown that the natural frequency Q_{nat} , which can be identified by $\text{Im}[\hat{\Delta}(Q_{nat})] = 0$, is shifted from Q_e and generates the misalignment with the zero crossing point of $\text{Re}[\hat{\Delta}(Q)] = 0$. A surprising consequence is then that the electromagnetic torque remains finite even at $Q = Q_{nat}$ as illustrated in Fig. 3. This implies that the magnetic islands remain finite and a torque balance remains always possible. If the size of magnetic islands is still smaller than nonlinear layer width, field penetration may be entirely prohibited.

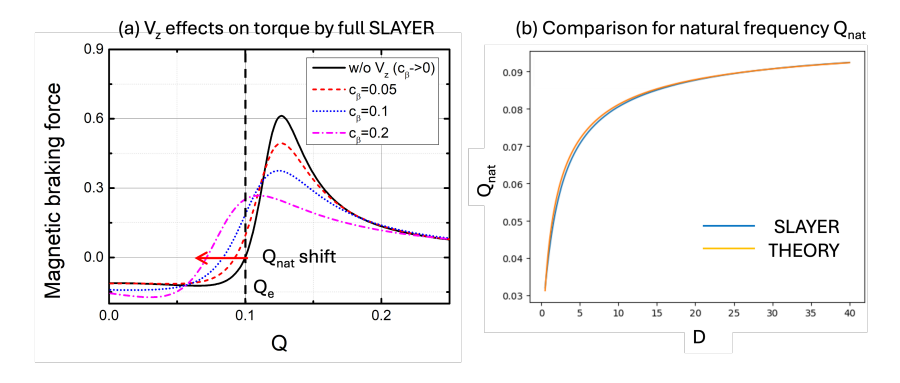


FIG. 3. (a) Reduced electromagnetic torque $\propto Im(1/\hat{\Delta})$ and natural frequency Q_{nat} shift due to ion parallel flow V_z when c_β increases, with the fixed $Q_e = -Q_i = 0.1$, P = 10, D = 1.0. (b) Comparison between full SLAYER calculations and analytic prediction for Q_{nat} .

This behavior is also reproduced by newly extended analytic theory. Retaining \bar{V}_z , Eq. (12) becomes

$$iQ\bar{Z} - iQ_e\bar{\phi} = -D^2 \frac{d^2(p^2\bar{\psi})}{dp^2} - c_\beta^2 p^2 \bar{Z} + c_\beta^2 \frac{d\bar{V}_z}{dp} + P_e D^2 p^4 (\bar{\phi} - \bar{Z}), \tag{24}$$

and adds the previously ignored equation

$$iQ\bar{V}_z + iQ_e\bar{\psi} = \frac{d\bar{Z}}{dp} - (P + P_e)p^2\bar{V}_z + P_e\frac{D^2}{c_o^2}p^4\bar{\psi}.$$
 (25)

The four-field equation can be arranged into a single 4th order ODE for $Y \equiv \bar{\phi} - \bar{Z}$ under the assumption that $P_e \ll (Q + Pp_*^2)^2/Pp_*^4$. The solution to this equation can be analytically treated by breaking three separate layers down in p-space where unique dominant balances occur as opposed to the two-layer matching technique for the three field model [6]. This method can be successfully applied to several regimes including HRi and SCi to predict a correction to $\hat{\Delta}$ which results in a shift in the natural frequency Q_{nat} from Q_e in agreement with numerical results from SLAYER. For example, the full form of the inner layer $\hat{\Delta}$ for the HRi regime is

$$\hat{\Delta}_{HRiVz} = i\pi (Q - Q_e) \left(2 \frac{\Gamma(3/4)}{\Gamma(1/4)} \left(\frac{c_{\beta}^2}{(1+\tau)D^2} \right)^{1/4} + (2^{7/4}) \frac{4}{5} \frac{\Gamma(13/8)}{\Gamma(3/8)} (1+\tau) P \frac{Q}{Q - Q_e} \left(\frac{c_{\beta}^2}{(1+\tau)D^2 P^2} \right)^{5/8} \right), (26)$$

where the second RHS term represents the correction from ion shielding effects. Fig. 3 (b) shows an excellent agreement between the numerical and analytic $\hat{\Delta}$ for the HRi regime.

4. FIELD PENETRATION SCALING PROJECTION AND VALIDATION

4.1. Scaling with operational parameters

The scaling of new regimes is aligned better with general observations, but in reality each asymptotic regime is not clearly isolated and experimental data points can lie in the transition or vary across the regimes. There are also two major uncertainties in the previous scaling. First is the assumption of zero $\vec{E} \times \vec{B}$ rotation, i.e. Q=0, which is not generally valid other than purely Ohmic plasmas. This assumption has been justified because error field data was initially populated largely in Ohmically heated cases. It is however necessary to predict the error field threshold in much wider parametric domains including L or H-modes with auxillary heating. Another uncertainty lies in the evaluation of viscosity, such as P or P_e . Scaling discussed by the previous section is obtained by assuming that momentum confinement time is roughly same as energy confinement time in Limited Ohmic Confinement (LOC) regime. However, viscosity can be easily anomalous and often better estimated by $P = \chi_{\phi}/(\eta/\mu_0)$ with χ_{ϕ} either from interpretive (or predictive) transport simulations or empirical values.

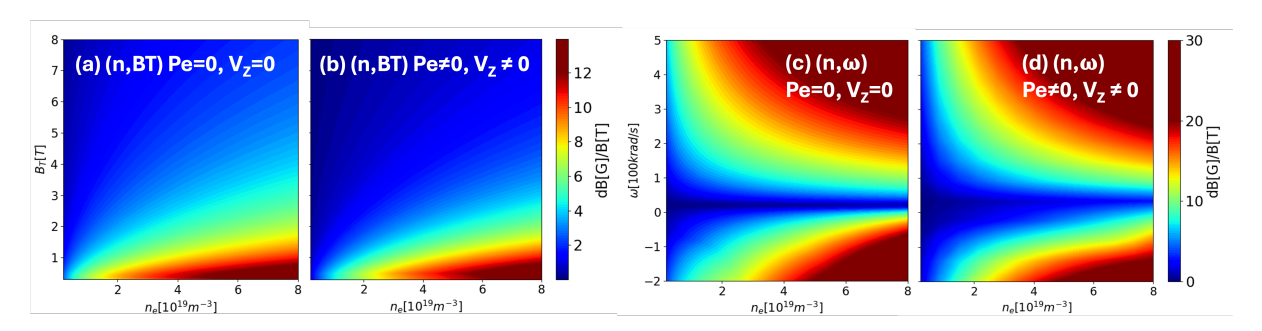


FIG. 4. Variation of field penetration threshold as a function (a,b) density and toroidal field, (c,d) density and rotation. (a,c) and (b,d) are without and with the electron viscosity and ion parallel flow.

So here we explored overall parametric scaling using SLAYER simulations, with and without electron viscosity + ion parallel flow to highlight the difference. Our focus is to variation of $\delta B/B_{\phi}$ as a function of n_e , B_T , and also rotation, in wide ranges while fixing other parameters. Fig. 4 shows the results for $3\times 10^{18}m^{-3} < n_e < 8\times 10^{19}m^{-3}, 0.3T < B_{\phi} < 8T$, and -20krad/s < $\omega_E < 50$ krad/s, with the $T_e = T_i = 1$ keV, $R_0 = 1.0$ m, $r_s = 0.5$ m, q = m/n = 2/1, $s = (r_s/q)(dq/dr) = 2.0$, $Z_{eff} = 2.0$, $\hat{\kappa} = 1.0$, and P = 3.0 and $P_e \cong P/60.0$. The positive density and negative B_{ϕ} scaling, as well as the positive scaling for the electron flow $\omega_{\perp,e} \equiv \omega + \omega_{e*}$ is also clearly represented. The modification by electron viscosity + ion parallel flow, (b,d) compared with (a,c), may be not so clear in the contour plot, but becomes apparent by regression analysis resulting in:

$$\delta_{OLD} \sim n^{0.56} B_{\phi}^{-0.75} \omega_{\perp,e}^{0.67} \longrightarrow \delta_{NEW} \sim n_e^{0.82} B_{\phi}^{-1.07} \omega_{\perp,e}^{0.79}. \tag{27}$$

4.2. Applications to locked mode database

Our analytic and numerical developments have been under investigations against experimental data points. Earlier SLAYER code without electron viscosity or ion parallel flow was already integrated with GPEC code package. GPEC can provide externally applied Δ due to EF or RMP to match $\Delta_{in} = \hat{\Delta}/\epsilon$ in Eq. (5) upon kinetic profile data as its first application was already attempted in [12]. Here we report another application of earlier version to q = 2/1 locked mode threshold data in Ohmically heated plasmas, especially when electron temperature data is available. Beam heated plasmas are excluded due to external momentum injection which can modify our torque balance model in slab. A successful example is shown in Fig. 5, with caveats about unknown local parameters such as $T_i = T_e$, P = 3.0, and Q = 0. Although this example illustrates a possibility to predict field penetration thresholds, experimental validation in the future must be carried out with accurate kinetic profiles and transport coefficients such as P or P_e , which our extended model is heavily dependent upon.

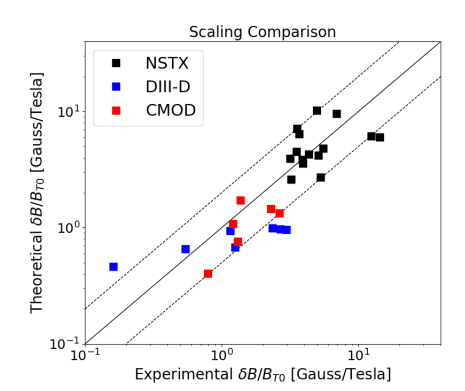


FIG. 5. Comparison of empirical field penetration threshold data with SLAYER based on slab torque balance, at the onset of locked modes in NSTX, DIII-D, CMOD ohmically heated plasmas.

5. CONCLUDING REMARKS

The two-fluid drift-MHD model has been successfully extended with electron viscosity and parallel ion flow. It is shown that electron viscosity can enhance positive density and negative toroidal field scaling for field penetration threshold, consistent with experiments despite the smallness of electron viscosity due to delicate balance in electron dynamics. Parallel ion flow perturbation becomes more important in higher β and can substantially shield resonant field along with shifted natural frequency. These new findings are shown analytically and verified by a full configuration solver as well as Riccati solver in momentum space, which are implemented in SLAYER code under GPEC code package. Experimental validations against error field and RMP database have been attempted, showing its prospect when accurate profile measurements or predictions are offered. Future work will also include the effects of neoclassical viscous effects, directly incorporating anisotropic tensor in drift-MHD layer equations, as its effects can be important in low collisionality conditions.

ACKNOWLEDGEMENTS

This work is supported by the Technology Development Projects for Leading Nuclear Fusion through the National Research Foundation of Korea (NRF) funded by the Ministry of Science and ICT (No. RS-2024-00281276), and also by US DOE under award No. DE-AC02-09CH11466 (Princeton Plasma Physics Laboratory) and No. DE-SC0022270 (Columbia University).

REFERENCES

- [1] R. Fitzpatrick and T. C. Hender. "The Interaction of resonant magnetic perturbations with rotating plasmas". In: *Phys. Fluids B* 3 (1991), pp. 644–673.
- [2] T. E. Evans et al. "Suppression of large edge-localized modes in high-confinement DIII-D plasmas with a stochastic magnetic boundary". In: *Phys. Rev. Lett.* 92 (2004), p. 235003.
- [3] J.-K. Park et al. "3D Field Phase-Space Control in Tokamak Plasmas". In: *Nat. Phys.* 14 (2018), pp. 1223–1228.
- [4] R. Fitzpatrick. "Bifurcated States of a Rotation Tokamak Plasma in the Presence of a Static Error-field". In: *Phys. Plasmas* 5 (1998), p. 3325.
- [5] R. Fitzpatrick and F. L. Waelbroeck. "Two-fluid Magnetic Island Dynamics in Slab Geometry". In: *Phys. Plasmas* 12 (2005), p. 022307.
- [6] A. J. Cole and R. Fitzpatrick. "Drift-magnetohydrodynamical Model of Error-field Penetration in Tokamak Plasmas". In: *Phys. Plasmas* 13 (2006), p. 032503.
- [7] R. Fitzpatrick. "Nonlinear error-field penetration in low density ohmically heated tokamak plasmas". In: *Plasma Phys. Control. Fusion* 54 (2012), p. 094002.
- [8] J. C. Waybright and J.-K. Park. "Effects of electron viscosity on resonant layer responses to non-axisymmetric magnetic perturbations". In: *Phys. Plasmas* 31 (2024), p. 022502.
- [9] Y. S. Lee, J. C. Waybright, and J.-K. Park. "Investigation of resonant layer response in electron viscosity regime". In: *Physics of Plasmas* 32.9 (Sept. 2025), p. 094501.
- [10] Y. S. Lee, J.-K. Park, and Y. S. Na. "Effect of parallel flow on resonant layer responses in high beta plasmas". In: *Nuclear Fusion* 64.10 (Sept. 2024), p. 106058.
- [11] J.-K. Park. "Parametric dependencies of resonant layer responses across linear, two-fluid, drift-MHD regimes". In: *Physics of Plasmas* 29.7 (July 2022), p. 072506.
- [12] N.C. Logan et al. "Metrics and extrapolation of resonant magnetic perturbation thresholds for ELM suppression". In: *Nuclear Fusion* 65.7 (June 2025), p. 076029.
- [13] R. Fitzpatrick. "Influence of anomalous perpendicular transport on linear tearing mode dynamics in tokamak plasmas". In: *Phys. Plasmas* 29 (2021), p. 032507.
- [14] I. Bandyopadhyay et al. "MHD, disruptions and control physics: Chapter 4 of the special issue: on the path to tokamak burning plasma operation". In: *Nuclear Fusion* 65.10 (Sept. 2025), p. 103001.
- [15] N. C. Logan et al. "Empirical scaling of the n=2 error field penetration threshold in tokamaks". In: *Nucl. Fusion* 60 (2020), p. 086010.